Counter Electrode Based on PEDOT:PSS - TiO_2 NTs Films for Dye-sensitized Solar Cells

RAMONA HULUBA[1], CRISTIAN PIRVU[1], CRISTINA NICOLESCU[2], MARIN GHEORGHE[3], MIHAELA MINDROIU[1]*

[1] University Politehnica of Bucharest, Faculty of Applied Chemistry and Materials Science, 1-7 Polizu Str., 011061, Bucharest, Romania

[2] Valahia University of Targoviste, 2 Carol I Blvd., 130024, Targoviste, Romania

[3] NANOM MEMS SRL, 9 G. Cosbuc Str., 505400, Rasnov, Brasov, Romania

A new dye-sensitized solar cell (DSSC) counter electrode was obtained through the electropolymerization of the monomer 3.4-Ethylendioxythiophene (EDOT) directly onto a indium tin oxide (ITO) coated glass in the presence of an aqueous titania nanotubes (TiO_2 NTs) suspension. The TiO_2 nanotubes in the anatase phase were incorporated in the conductive polymer film, being also observed an increase in the catalytic activity and the fill factor of the assembled device when using the under examination counter electrode.

Keywords: TiO_2 nanotubes suspension, PEDOT:PSS, Dye-sensitized solar cells

The interest in the development of dye-sensitized solar cells (DSSCs) increased since 1991 [1], when O'Regan and Grätzel assembled the first DSSC based on TiO_2 nanoparticles sensitized with Ru-dyes, a platinum (Pt) counter electrode and iodine based electrolyte [1, 2]. The technology of DSSCs has shown impressively fast scientific progress due to its many advantages, which also stand for its future potential as part of the generally acknowledged renewable energy sources, namely the photovoltaic systems. One particularly significant improvement in the manufacture of these solar cells is that they are low cost and simple [3, 4]. Usually the working electrode of a DSSC is composed of TiO_2 in anatase phase with nanoporous structure, in order to increase the inner surface, which leads to a higher photoconversion efficiency. Moreover, for good performances of DSSCs, both high conductivity and catalytic activity of the counter electrode (CE) are mandatory. The most frequently used metal for the CE is platinum due to its catalytic activity [5] but it has a major disadvantage, namely the high price. A wide variety of alternative conductive materials, such as graphene, graphite, aluminum or conductive polymers [6-8] are used as CE [9-13]. Among the conducting polymers with good catalytic activity and conductivity used as the CE in DSSCs is PEDOT:PSS [14]. The conducting polymers can be easily deposited onto ITO and metallic substrates by electrochemical polymerization of the monomer in presence of surfactants, using both organic and aqueous solutions, as we already shown in a previous work [15]. In the latest studies the interest in anodic polymerization of EDOT by using aqueous solvent rose, as it is low-priced and less toxic than organic solutions [16-19].

However, because of the low energy conversion efficiency of pure PEDOT in comparison to Pt [20-22], methods to enhancing the active area are investigated. These methods consist in the incorporation of different materials in the polymer solution, for instance grapheme [23] or carbon nanotubes [24]. Another method was proposed by Wasan Maiaugree et al, who mixed TiO_2 nanoparticles with a PEDOT:PSS solution [14]. In their report, they have proved that the efficiency of the solar cell has improved and that it depends on the dimensions of the TiO_2 nanoparticles.

In our work, a PEDOT:PSS film was electrodeposited onto ITO in presence of a suspension of aqueous titania nanotubes (TiO_2 NTs) in order to increase the surface area and catalytic activity of the polymeric film. Due to these properties and a great length-to-diameter ratio, the dye absorption and the electron transportation are increased, making TiO_2 NTs widely used in the production of solar cells for the electrodes [25-27]. The TiO_2 NTs suspension can be easily and low-cost obtained through the anodization method with platinum foil used as the cathode in the presence of a solution which contains flour ions [28-30].

Experimental part

Preparation and characterization of the TiO_2 NTs suspension

Firstly, the amorphous TiO_2 nanotubes arrays were obtained by the anodization of commercially pure Ti electrodes with 10 mm diameter and 1 mm thickness (99.6% purity grade 2, Goodfellow Cambridge Ltd., UK). After polishing the Ti foils to a mirror like surface with silica carbide paper in different grain sizes between grit 320 to 4000, they were successively ultrasonically degreased in ethanol, acetone and deionized water, for 15 min in each solution, at room temperature. A two-electrode configuration was used for the anodic oxidation, with platinum foil as the cathode. The anodization was carried out at the constant potential of 55 V. This applied voltage was reached with a rate of 2 V / 10 s. using a MATRIX MPS-7163 electrochemical source, and the anodization time was 2 h. The anodization bath is made of ethylene glycol ($C_2H_6O_2$ for analysis, with 99.5 % of purity, Merck) containing NH_4F 0.5 wt% (Merck) and a small amount of water 2% H_2O (in volume) [31].

The titania nanotubes arrays obtained in a fluoride based solution were first reported in 2001 by Grimes et al. [32], and in ethylene glycol solution were attained by Dumitriu et al. [33]. The mechanism of the TiO_2 NTs synthesis by the anodization of Ti foils as a result of the competition between electrochemical oxidation and chemical dissolution was already explained in a our previous work [28]. In order to use TiO_2 NTs in DSSC applications, the amorphous electrode was annealed at 500°C in a furnace for 30 min to reach the anatase phase of the TiO_2 NTs,

*email: m_mindroiu@chim.upb.ro; Tel.: +4021 402 39 30

which was proved to have higher catalytic activity [34] and electron mobility [35]. The anatase TiO_2 NTs were detached from the Ti substrate by an ultrasonication process in a mixture (1:1) of deionized water and poly ethylene glycol (PEG) 400 g/mol. The addition of PEG is necessary to stabilize the obtained titania nanotubes suspension. The final concentration of TiO_2 NTs in the suspension was 6.5%. The crystalline nature of the TiO_2 nanotubes annealed at 500 °C was analyzed using a Rigaku Ultima IV X-ray diffractometer (XRD) in Bragg Brentano para-focusing setup with high resolution, using CuKα radiation (λ=0.154nm). The source was operated at 40 kV and 40 mA. The morphology and the lengths of the TiO_2 NTs in suspension were determinate by Scanning Electron Microscopy (SEM) technique using a FEI Nova NanoSEM 630 FEG-SEM (SEM with Field Emission Gun) system with ultra-high resolution characterization at high and low voltage in high vacuum.

Electrosynthesis and characterisation of the PEDOT:PSS and PEDOT:PSS-TiO_2NTs films on ITO electrodes, used as counter electrodes for DSSC

Before the electrodeposition phase, the ITO electrodes were washed successively in Triton X-100, ethyl alcohol and distilled water. The electrodeposition was done through the CV method by applying a voltage domain between -0.5 V and 1.8 V versus the Ag/AgCl refference electrode, the scanning rate being 50 mV/s for 4 cycles. The materials used for preparing the aqueous solution were: 0.01 M EDOT monomer solution (Aldrich), 0.1 M KNO_3, 0.1 M NaPSS, with/without TiO_2 NTs suspension with a concentration of aproximatively 0.5 % TiO_2.

The FT-IR analyses for the PEDOT:PSS and PEDOT:PSS-TiO_2NTs films were conducted with Spectrum 100 PerkinElmer equipment using diamond ATR technique. The scanning was ranged from 4000 cm^{-1} to 600 cm^{-1}.

The PEDOT:PSS/ITO and PEDOT:PSS-TiO_2NTs/ITO obtained electrodes were electrochemically characterized, in order to evaluate their capacity to be used as counter electrodes for DSSCs. The catalytic activity of the film with I^-/I_3^- was measured by CV in a three compartment cell at a scan rate of 20 mV/s in 10 mM LiI, 1 mM I_2 and 0.1 M $LiClO_4$ in an acetonitrile (ACN) solution, the voltage domain being -0.2 V ÷ 1 V. The active area of the PEDOT:PSS/ITO and PEDOT:PSS-TiO_2NTs/ ITO counter electrodes was analyzed by CV in a 1 mM $K_3Fe(CN)_6$ and 0.1 M KCl aqueous solution in the three-compartment cell at a scan rate of 5, 10, 20, 50, 100, 200, 300 and 500 mV/s.

DSSC assembly

The crystallized working electrode was prepared by depositing a mixture from Titanium (IV) oxide (anatase powder, < 25 nm, 99.7% metals basis, Sigma Aldrich) and TiO_2 NTs suspension onto ITO and then, annealed at 500°C for 1 h. The sensitization of the TiO_2 based photoanode was achieved in a solution of N719 dye for 24 h. Two DSSCs were assembled by sandwiching a sensitized WE and a CE, PEDOT:PSS/ITO and PEDOT:PSS-TiO_2NTs/ITO, respectively. A hole was realized in the counter electrode, through which the 0.1 M LiI, 0.01 M I_2, 20 vol% NMP (N-metil pirolidinã) in 80 % ACN electrolyte was introduced. The I-V characteristics of the two DSSCs were measured using an AUTOLAB PGSTAT 302N potentiostat/galvanostat in a ULTRA-LUM, INC. Carson, California 90746 (230 V; 50 Hz; 1 A) source illumination at 365 nm.

Results and discussions

Characterization of the TiO_2 NTs suspension

The morphology and dimensions of the TiO_2 nanotubes in suspension of a PEG 400 solution are illustrated in figure 1.

The anodization of the titanium in a fluoride based solution leads to the formation of self-organized TiO_2 nanotubes [28], and after annealed at 500°C for 30 min and then detached from the Ti substrate by an ultrasonication process in a PEG 400 solution, the nanotubular structure is conserved, according to figure 1.

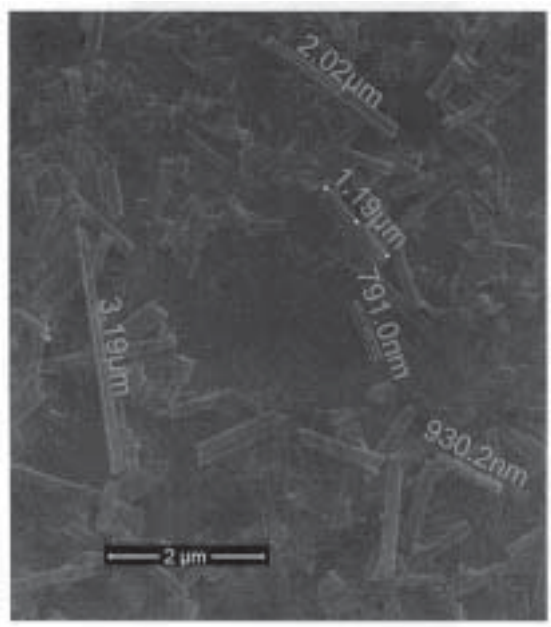

Fig. 1. The SEM image of TiO_2 nanotubes in suspension

Also, the most of the TiO_2 nanotubes have the lengths between 0.7 and 4µm.

Moreover, the anatase phase of the TiO_2 nanotubes annealed at 500°C for 30 min was highlighted in figure 2. The XRD pattern of the heat treated TiO_2 nanotubes was registered from 10-120 degrees, 2θ/θ scan axis, with 0.02° angular step and 0.5 s/step. The resulting pattern revealed the formation of well-crystallized single anatase phase. The TiO_2 NTs exhibit lines that correspond to anatase crystal planes (101), (004), (112), (200), (105), (211), (204), (116), (220), (215) and (312). No extra peaks corresponding to any other secondary phases are observed.

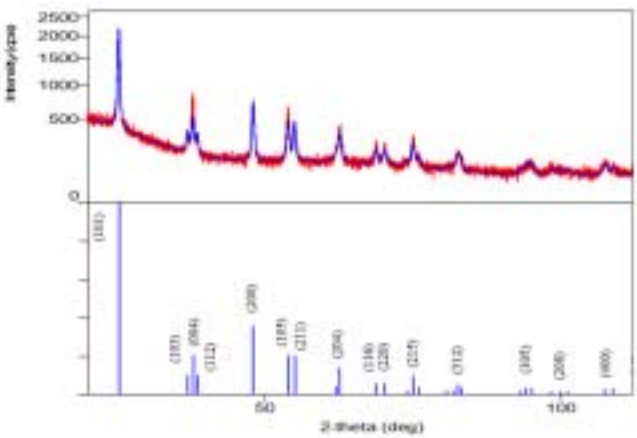

Fig. 2. XRD diffraction patterns of TiO_2 NTs annealed at 500 °C for 30 min.

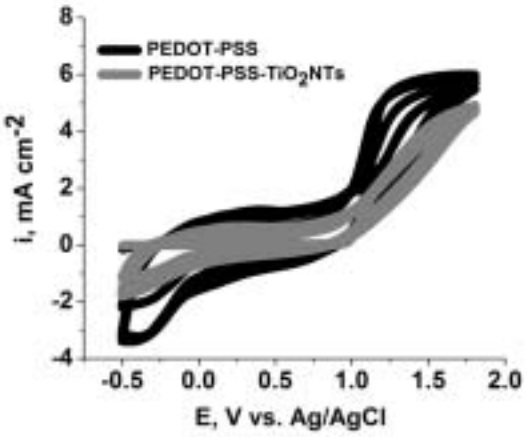

Fig. 3. Potentiodynamic curves of the PEDOT:PSS film and PEDOT:PSS-TiO_2NTs film electrodeposited onto ITO

Electrodeposition of the PEDOT:PSS and PEDOT:PSS-TiO_2NTs films onto ITO electrodes

The electrodeposition of the polymeric films is depicted in figure 3.

In figure 3 it can be observed that the polymer films were electrodeposited onto ITO in both cases, with/without the titania nanotubes suspension, as the values for the current density increased with the number of cycles. When using the TiO_2 NTs suspension in the electropolymerization solution, the oxidation pick of the polymer is deviated from 1.1 V corresponding to pure PEDOT:PSS to a more positive value of 1.4 V. In both cases, the polymer films were continuous, adherent onto the ITO substrate and having a black color. These electrodes were designed in order to be used as counter electrodes for DSSCs.

Characterization of the obtained counter electrodes

Structure characterization

To prove the integration of the TiO_2 NTs in the aqueous suspension with PEG, the FT-IR spectra of the TiO_2NTs-PEG 400 aqueous suspension, and for the PEDOT:PSS and also for the PEDOT:PSS-TiO_2NTs films electrodeposited on ITO electrodes were investigated (fig. 4).

The FT-IR spectrum of the hybrid composite PEDOT:PSS-TiO_2NTs suspension proves that the TiO_2 nanotubes, which are mixed with PEG 400, are incorporated in the mesh of the conductive polymer PEDOT:PSS. The functional group corresponding to TiO_2 at 685 cm^{-1} appears in the FT-IR spectrum of the TiO_2 NTs - PEG 400 suspension and of the composite. The C-O-C bound, which is characteristic of PEG 400, is present in the

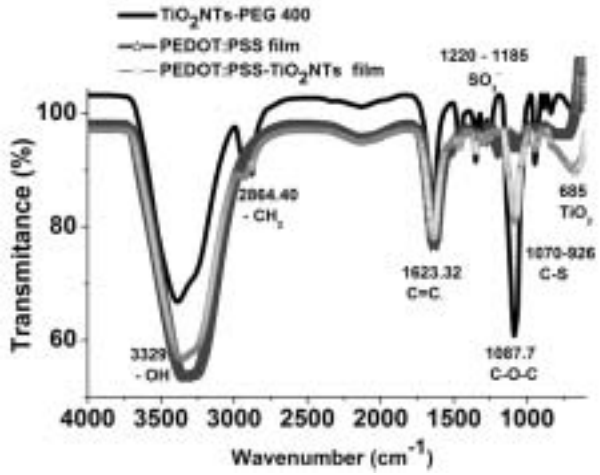

Fig. 4. The FT-IR spectra of the TiO_2NTs-PEG 400 aqueous suspension, and of the PEDOT:PSS film and of the PEDOT:PSS-TiO_2NTs film

spectrum of the composite, having the peak at 1087.7 cm^{-1}. Functional groups corresponding to the polymer can be identified in the spectrum of the composite. For instance, the peak at 1623.32 cm^{-1} is matching the C=C bond, while the interaction C-S in the thiophene ring can be identified by the bands at 1070 ÷ 926 cm^{-1}. The bands matching the absorption of SO_3^- in the NaPSS group are in the 1220 - 1185 cm^{-1} region and appear in the FT-IR spectrum of both PEDOT:PSS and the composite PEDOT:PSS-TiO_2NTs-PEG 400. The peak corresponding to stretching vibrations of the functional group - OH is present in all of the spectra at around 3329 cm^{-1}.

Electrochemical characterization

The performance of the counter electrodes, where the TiO_2 NTs suspension was added, could possibly be attributed to the active area and catalytic activity [14]. To analyze the catalytic activity of the film the CV was conducted in 10 mM LiI, 1 mM I_2, and 0.1 M $LiClO_4$ acetonitrile solution. The results are presented in figure 5.

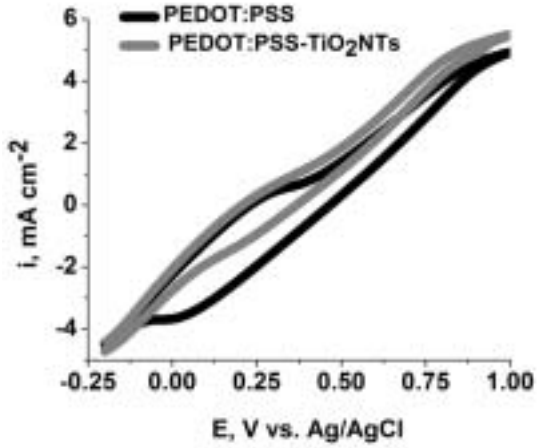

Fig. 5. The cyclic voltammogram curves of PEDOT:PSS/ITO and of composite PEDOT:PSS-TiO_2NTs/ITO at a scan rate of 20 mV/s in 10 mM LiI, 1 mM I_2, and 0.1 M $LiClO_4$ in ACN solution

From figure 5 it can be seen that the reduction peak of composite films significantly increased from 0.4 mA to 0.6 mA after the addition of TiO_2NTs suspension. This result implies that nanotubes suspension promote polymer film catalytic activity, as expected. Furthermore, comparing the reduction positions, the pure PEDOT:PSS film has higher reduction voltages (~ 0.31 V) than the composited PEDOT:PSS-TiO_2NTs (~ 0.26 V). This behavior indicates that the suspension presence enlarges the film active area and/or decreases the film resistance.

Also, in order to estimate the polymer film active area, the current versus applied voltage at different scanning rates of the PEDOT:PSS/ITO and PEDOT:PSS-TiO_2NTs/ITO electrodes in a 1 mM $K_3Fe(CN)_6$ and 0.1 M KCl solution is described in figure 6.

In both cases, the current value increases with scanning rate. The presence of the nanotube suspension in polymer film leads to a higher current value than that of the pure polymer film, which indicates a more intense catalytic activity.

The real active areas of the PEDOT:PSS/ITO and PEDOT:PSS-TiO_2NTs/ITO electrodes were determined using the Randles-Sevcik equation from CVs curves:

$$Ip = 2.72\times10^5\times n^{3/2}\times A\times D^{1/2}\times v^{1/2}\times C \quad (1)$$

where Ip is the peak current (A), n (=1) is the number of electrons transferred, A is the effective area of the electrode (cm^2), D is the diffusion coefficient of $[Fe(CN)_6]^{3-}$ (taken to

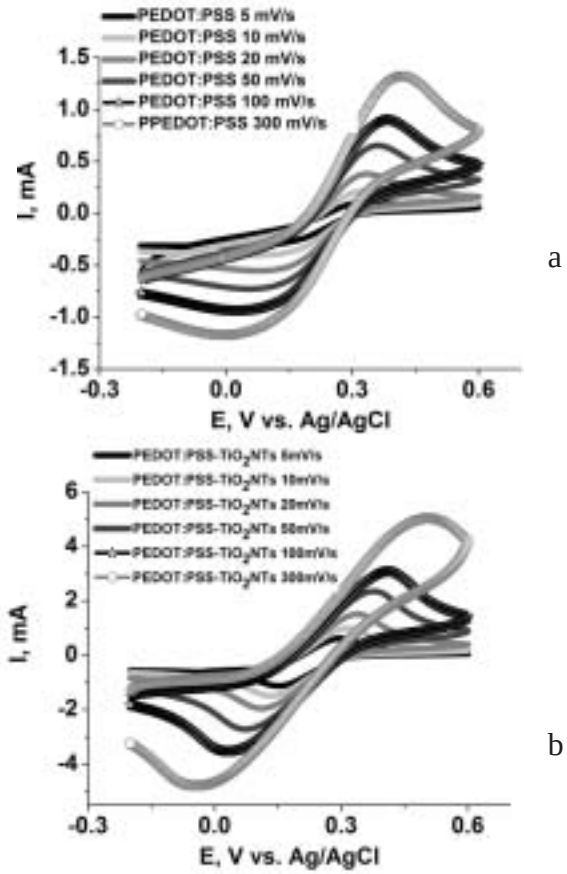

Fig. 6. CV curves for: (a) PEDOT:PSS/ITO and (b) PEDOT:PSS-TiO_2NTs/ITO electrodes at different scan rates in the 1 mM $K_3(FeCN)_6$ and 0.1 M KCl solution

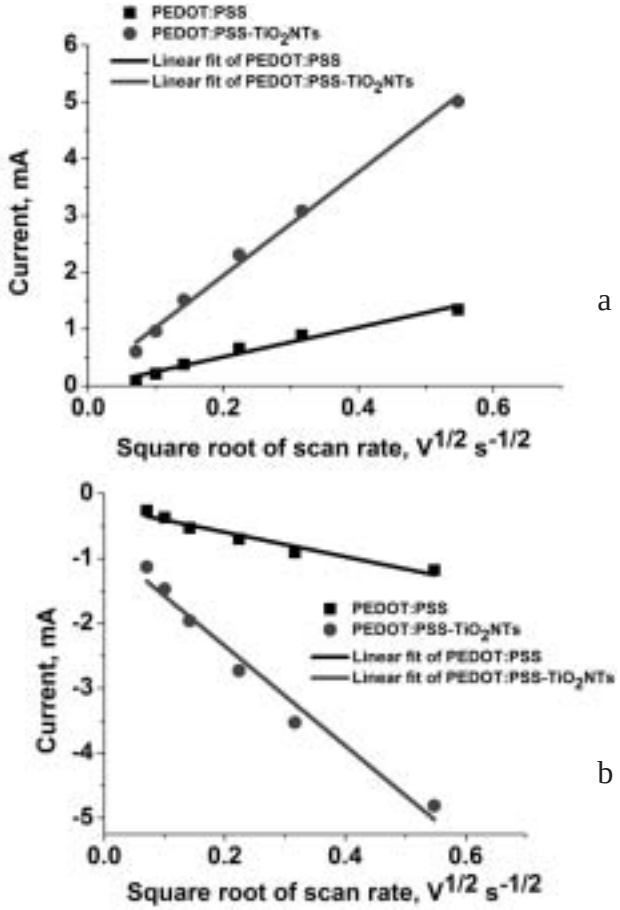

Fig. 7. Randles - Sevcik plots of: (a) the reduction and (b) the oxidation current of $[Fe(CN)_6]^{3-}$ vs. the square root of the scan rate ($v^{1/2}$) and their fittings

be 7.60 x 10^{-6} cm^2 . s^{-1}), C is the concentration (mol . cm^{-3}), v is the scan rate (V s^{-1}).

The reduction and oxidation current of $[Fe(CN)_6]^{3-/4-}$ vs. the square root of the scanning rate ($\nu^{1/2}$) for the PEDOT:PSS/ITO and PEDOT:PSS-TiO_2NTs/ITO electrodes were calculated and fitted in figure 7.

Figure 7 shows a linear dependence between the reduction and the oxidation current of $[Fe(CN)_6]^{3-}$ vs. the square root of the scan rate ($\nu^{1/2}$), indicates a reversible redox process at the electrode surface. According to literature [14], the TiO_2 NTs does not react with $[Fe(CN)_6]^{3-}$ and the slope of Current - $\nu^{1/2}$ curves varies only with the film active area.

The active area for PEDOT:PSS-TiO_2NTs/ITO electrode, calculated with equation 1, is about 12.3 cm^2, while for PEDOT:PSS/ITO electrode is 3.5 cm^2. These results sustain the probability of polymerization of EDOT-PSS around the TiO_2 NTs, leading to a higher active area.

Measurement of the front illuminated DSSCs

DSSCs were assembled using PEDOT:PSS/ITO and PEDOT:PSS-TiO_2NTs/ITO as counter electrodes. Figure 8 shows the photocurrent density (I) - photovoltage (V) and power - voltage (P-V) characteristic of DSSCs assembled.

From the I-V and P-V curves, the following parameters were extracted: I_{SC}(short-circuit current) is the cell current measured at an applied potential of 0 V, V_{OC} (open-circuit voltage) is the cell potential measured when the current is 0 A, P_{max} (maximum power point) is the point where the maximum power is generated. The FF (fill factor) is calculated according to the equation 2:

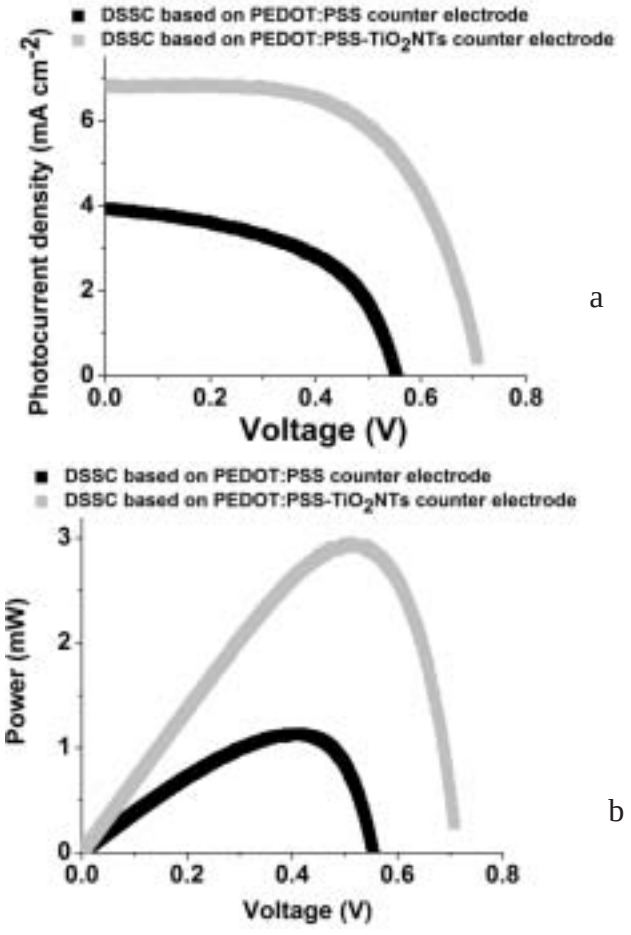

Fig. 8. (a) I-V and (b) P-V curves recorded at 365 nm

Sample	I_{SC} (mA cm^{-2})	V_{OC} (V)	P_{max} (mW)	FF (%)
DSSC based on PEDOT:PSS counter electrode	3.925	0.550	1.12	0.51
DSSC based on PEDOT:PSS-TiO_2NTs counter electrode	6.808	0.752	2.92	0.57

Table 1
THE PARAMETERS OF THE PHOTOVOLTAIC PERFORMANCE OF THE STUDIED DSSCs

$$FF = \frac{P_{max}}{V_{oc} \times I_{sc}} \quad (2)$$

In table 1 the main parameters calculated from I-V and P-V curves are presented.

P_{max} and FF parameters corresponding to DSSC assembled with PEDOT:PSS-TiO_2NTs/ITO as CE have higher values compared to DSSC which contains PEDOT:PSS/ITO as CE. The presence of the TiO_2 NTs suspension in the polymeric film improves the photovoltaic performance of the DSSC.

Conclusions

The TiO_2 nanotubes were incorporated in the PEDOT:PSS film, which was obtained by electropolymerization of EDOT monomer solution in the presence of titania nanotubes suspension. This result was emphasized by the FT-IR data. The CVs have shown that the active surface and the catalytic activity of the PEDOT:PSS-TiO_2NTs based contra electrode (CE) were improved. The DSSC assembled, which had both the WE and the CE doped with the TiO_2NTs suspension, has shown better performance than the one without the nanotubes suspension at the CE. I-V and P-V curves come in support of this statement.

References

1.O' REGAN, B., GRÄTZEL, M., Nature, **353,** 1991, p. 737–740.
2.BRADSHAW, A. M., HAMACHER, T., ChemSusChem, **5**, nr. 3, 2012, p. 550–562.
3.KAMAT, P. V., The Journal of Physical Chemistry C, **111**, nr. 7, 2007, p. 2834–2860.
4.YU, M., LONG, Y. Z., SUN, B., FAN, Z., Nanoscale,. **4**, nr.9, 2012, p. 2783–2796.
5.YOON, C. H., VITTAL, R., LEE, J., CHAE, W. S., KIM, K. J., Electrochimica Acta, **53**, nr. 6, 2008, p. 2890–2896.
6.ZHANG, J., HREID, T., LI, X., GUO, W., WANG, L., SHI, X., SU, H., YUAN, Z., Electrochimica Acta, **55**, nr. 11, 2010, p. 3664–3668.
7.TAI, Q., CHEN, B., GUO, F., XU, S., HU, H., SEBO, B., ZHAO, X. Z., ACS Nano, **5**, nr. 5, 2011, p. 3795–3799.
8.JO, Y., CHEON, J. Y., YU, J., JEONG, H. Y., HAN, C. H., JUN, Y., JOO, S. H., Chemical Communications, **48**, nr. 65, 2012, p. 8057–8059.
9.LI, G. R., WANG, F., JIANG, Q. W., GAO, X. P., SHEN, P. W., Angewandte Chemie International Edition., **49**, nr. 21, 2010, p. 3653–3656.
10.HAN, J., KIM, H., KIM, D. Y., JO, S. M., JANG, S. Y., ACS Nano, **4**, nr. 6, 2010, p. 3503–3509.
11.PALMAS, S., DA POZZO, A., MASCIA, M., VACCA, A., RICCI, P. C., Chemical Engineering Journal, **211**, 2012, p. 285–292.
12.MURAKAMI, T. N., ITO, S., WANG, Q., NAZEERUDDIN, M. K., BESSHO, T., CESAR, I., LISKA, P., HUMPHRY-BAKER, R., COMTE, P., PÉCHY, P., GRÄTZEL, M., Journal of The Electrochemical Society, **153**, nr.12, 2006, p. A2255–A2261.
13.SUN, H., LUO, Y., ZHANG, Y., LI, D., YU, Z., LI, K., MENG, Q., The Journal of Physical Chemistry C, **114**, nr. 26, 2010, p. 11673-11679.
14.MAIAUGREE, W., PIMANPANG, S., TOWANNANG, M., SAEKOW, S., JARERNBOON, W., AMORNKITBAMRUNG, V., Journal of Non-Crystalline Solids, **358**, nr. 17, 2012, p. 2489–2495.
15.MINDROIU, M., PÎRVU, C., POPESCU, S., DEMETRESCU, I., Mat. Plast., **46,** no. 4, 2009, p. 394-398.
16.PATRA, S., BARAI, K., MUNICHANDRAIAH, N., Synthetic Metals, **158**, nr. 10, 2008, p. 430–435.
17.WEN, Y., XU, J., HE, H., LU, B., LI, Y., DONG, B., Journal of Electroanalytical Chemistry,. **634**, nr. 1, 2009, p. 49–58.
18.TAMBURRI, E., ORLANDUCCI, S., TOSCHI, F., TERRANOVA, M. L., PASSERI, D., Synthetic Metals, **159**, nr. 5, 2009, p. 406-414.
19.ZHOU, C., LIU, Z., DU, X., RINGER, S. P., Synthetic Metals, **160**, nr. 15, 2010, p. 1636–1641.
20.MUTO, T., IKEGAMI, M., KOBAYASHI, K., MIYASAKA, T., Chemistry Letters, **36**, nr. 6, 2007, p. 804–805.
21.MUTO, T., IKEGAMI, M., MIYASAKA, T., Journal of The Electrochemical Society, **157**, nr. 8, 2010, p. B1195–B1200.
22.ANDRADE, L., RIBEIRO, H.A., MENDES, A., Dye-sensitized solar cells: an overview, in Encyclopedia of Inorganic and Bioinorganic Chemistry 2011, p. 1–20.
23.HONG, W., XU, Y., LU, G., LI, C., SHI, G., Electrochemistry Communications, **10**, nr. 10, 2008, p. 1555–1558.
24.FAN, B., MEI, X., SUN, K., OUYANG, J., Applied Physics Letters, **93**, nr. 14, 2008, p. 143103.
25.MOR, G. K., SHANKAR, K., PAULOSE, M., VARGHESE, O. K., GRIMES, C. A., Nano Letters, **6**, nr. 2, 2006, p. 215–218.
26.ZHU, K., NEALE, N. R., MIEDANER, A., FRANK, A. J., Nano Letters, **7**, nr. 1, 2007, p. 69-74.
27.LI, D., LIN, S., LI, S., HUANG, X., CAO, X., LI, J., Journal of Materials Research, **27**, nr. 7, 2012, p. 1029–1036.
28.MÎNDROIU, M., PIRVU, C., ION, R., DEMETRESCU, I., Electrochimica Acta, **56**, nr. 1, 2010, p. 193-202.
29.DUMITRIU, C., POPESCU, M., VOICU, G., DEMETRESCU, I., Rev. Chim. (Bucharest), **64**, no. 6, 2013,p. 599-602.
30.ROY, P., BERGER, S., SCHMUKI, P., Angewandte Chemie International Edition, **50**, nr. 13, 2011, p. 2904–2939.
31.MOHAPATRA, S. K., RAJA, K. S., MAHAJAN, V. K., MISRA, M, The Journal of Physical Chemistry C, **112**, nr. 29, 2008, p. 11007–11012.
32.GONG, D., GRIMES, C. A., VARGHESE, O. K., HU, W., SINGH, R. S., CHEN, Z., DICKEY, E. C., Journal of Materials Research, **16**, nr.12, 2001, p.3331–3334.
33.DUMITRIU, C., PIRVU, C., DEMETRESCU, I., Journal of The Electrochemical Society, **160**, nr. 2, 2013, p. G55-G60.
34.PARK, N. G., VAN DE LAGEMAAT, J., FRANK, A. J., The Journal of Physical Chemistry B, **104**, nr. 38, 2000, p. 8989–8994.
35.TIGHINEANU, A., RUFF, T., ALBU, S., HAHN, R., SCHMUKI, P., Chemical Physics Letters, **494**, nr.4, 2010, p. 260–263.

Manuscript received: 21.09.2015